

A Novel Direct Torque Control for Electrically Excited Synchronous Motor Drives with High Power Factor and Low Ripples in Flux and Torque

Yangzhong Zhou* and Yuwen Hu**

* Fuzhou University, Fuzhou, China, Email: zhty_75313@sina.com

** Nanjing University of Aeronautics and Astronautics, Nanjing, China

Abstract—A direct torque control (DTC) method for electrically excited synchronous motor (ESM) drives has been investigated in this paper. It is based on the compensation of the stator flux linkage vector error using the space vector modulation to decrease the ripples in torque and flux linkage. In order to increase the power factor and load ability of ESMs, an optimum rotor field current control scheme has been presented, which is suited well in the whole speed range. In the closed loop of the rotor current control, the reference rotor current is directly calculated with the torque and stator flux linkage modulus references. Compared to the traditional DTC method, the results of experiments show that the presented DTC has low ripples in torque and flux linkage, and almost achieves unity power factor.

Keywords—Electrically excited synchronous motor, Direct torque control, Space vector modulation, Rotor field current, Power factor

I. INTRODUCTION

The direct torque control (DTC) theories for electrically excited synchronous motor (ESM) drives were researched partly by Switchland researchers in about 1998^[1-2]. The inductance value of ESM is small, and the dynamic inductance value is even low in ESM because of the damper windings on the rotor. The ripples in torque and stator flux linkage may be high, and the stability of drive system may be affected, if the basic DTC with stator flux linkage and torque hysteresis controllers is applied into ESM drives. In order to decrease these ripples, a number of feasible methods were investigated for the DTC inductance motor (IM) drives and permanent synchronous motor (PMSM) drives. Recently, many researchers' efforts have been given to the DTC scheme with space vector modulation (SVM)^[3-9]. Although many SVM-DTC schemes were investigated intensively for IM and PMSM, the SVM-DTC scheme for ESM has not been presented.

Many ESMs are applied in industry because of their advantages such as good dynamic performance, adjustable power fact and high efficiency, and thus it is very valuable to research the ESM SVM-DTC. Although ESM and PMSM are all synchronous motor, the excited winding and damper windings mounted on the ESM rotor make the ESM torque control principle different from that of

PMSM, and so it is very necessary to research the ESM SVM-DTC.

II. TORQUE CONTROL PRINCIPLE OF SVM-DTC ESM DRIVES

In an ESM, the electromagnetic torque T_e can be calculated as the cross product of the stator flux linkage vector and the air gap flux linkage vector^[10]

$$T_e = \frac{3}{2L_{s\sigma}} p \boldsymbol{\varphi}_s \times \boldsymbol{\varphi} = \frac{3}{2L_{s\sigma}} p |\boldsymbol{\varphi}_s| |\boldsymbol{\varphi}| \sin \theta \quad (1)$$

Where

$\boldsymbol{\varphi}_s, \boldsymbol{\varphi}$ - stator and air gap flux linkage vector,

$L_{s\sigma}$ - stator leakage inductance,

P - pole pairs,

θ - torque angle i.e. the angle between $\boldsymbol{\varphi}_s$ and $\boldsymbol{\varphi}$.

The air gap flux linkage has quite a long time constant due to different damping effects in the air gap region, typically in the range of 10..100ms, which is quite larger than the system sampling period T_s , and so the space position of air gap flux linkage vector in d-q rotor rotation frame is almost not changed in a fast transient. T_e can be modulated quickly with the fast torque angle change, by rotating the stator flux linkage vector based on the above characteristic of the air gap flux linkage.

Fig.1 shows the torque control principle of EMS SVM-DTC system, in which the stator winding resistances are neglected and it is assumed that the stator flux linkage vector is $\boldsymbol{\varphi}_{sk}$ when the k^{th} sampling period is over. The required stator flux linkage vector $\boldsymbol{\varphi}_{sk+1}$ in the $k+1^{\text{th}}$ sampling period is anticipated with torque error ($T_e^* - T_e$) and the given stator flux linkage vector modulus φ_s^* , and the stator flux linkage error vector $\Delta \boldsymbol{\varphi}_{se}$ can be calculated from $\boldsymbol{\varphi}_{sk+1}$ and the actual stator flux linkage vector $\boldsymbol{\varphi}_{sk}$. When the SVM method is considered, the V_6, V_2 and V_0 voltage vectors are selected, working with T_1, T_2 and T_0 ($T_0 = T_s - T_1 - T_2$) respectively in a sampling period T_s in order to cancel the stator flux linkage error vector $\Delta \boldsymbol{\varphi}_{se}$, and then the torque and stator flux linkage vector are controlled exactly and quickly.

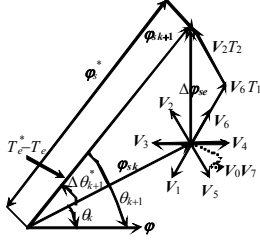


Figure 1. The control principle for torque and stator flux linkage

III. OPTIMUM ROTOR FIELD CURRENT CONTROL STRATEGY IN DTC ESM DRIVES

A control strategy of optimum rotor field current for the air gap flux linkage oriented vector control ESMs has been presented by some researchers as shown in Fig.2. The main idea is to control the field current with unity outer power factor below a speed n_s , called the outer control strategy, and with unity inner power factor above the nominal speed n_N , called the inner control scheme, and to keep the stator voltage with nominal value within the rotor rotating speed between $n_s \dots n_N$. The rotor current reference is calculated with the flux current component and torque current component.

There are two closed loop controls i.e. stator flux linkage and torque, and no current controls are necessary in the DTC drives. Thus the above rotor field current control method can not be applied into the DTC ESM drives directly.

A. Inner Control Strategy of Rotor Current

The vector diagram with unity inner power factor is shown in Fig.3, where e_s , e and u_s are the stator induced electro motive force vector, back electro motive force vector and terminal voltage vector respectively, Φ_e is the outer power factor angle between the stator current i_s and stator voltage u_s , δ is the load angle between the stator flux linkage ϕ_s and rotor d-axis, R_s is the stator resistance, and ω is the rotating electrical angle speed of rotor. The i_s is in phase with the e to keep with unity inner power factor.

The rotor current can be expressed as a function of the torque and the stator flux linkage modulus based on the vector relation as shown in Fig.3

$$i_f = \frac{(3p\phi)^2 + 4L_{md}L_{mq}\left(\frac{T_e}{\phi}\right)^2}{3pM_{sf}\sqrt{(3p\phi)^2 + \left(\frac{2L_{mq}T_e}{\phi}\right)^2}} \quad (2)$$

$$\phi = \sqrt{\frac{\phi_s^2 + \sqrt{\phi_s^4 - \left(\frac{4T_e L_{sq}\sigma}{3p}\right)^2}}{2}} \quad (3)$$

Where

L_{md} , L_{mq} - d-axis and q-axis magnetising inductance respectively,

M_{sf} - mutual inductance between d-axis stator winding and rotor winding.

B. Outer Control Strategy of Rotor Current

The vector diagram with unity outer power factor is shown in Fig.4, where Φ_i is the inner power factor angle between i_s and e . i_s is in phase with u_s to keep with unity outer power factor.

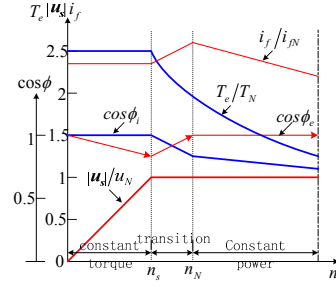


Figure 2. The optimum rotor current control strategy for vector controlled ESMs

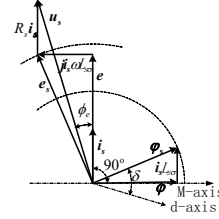


Figure 3. The vector diagram with unity inner power factor

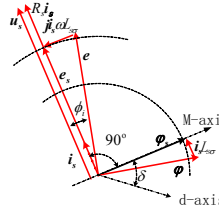


Figure 4. The vector diagram with unity outer power factor

After analysed intensively, the rotor current is expressed as

$$i_f = \frac{(3p\phi_s)^2 + 4L_dL_q\left(\frac{T_e}{\phi_s}\right)^2}{3pM_{sf}\sqrt{(3p\phi_s)^2 + \left(\frac{2L_qT_e}{\phi_s}\right)^2}} \quad (4)$$

Where

L_d , L_q - d-axis and q-axis inductance respectively.

C. Optimum Control Strategy of Rotor Current

The parameters of ESM are shown in Table 1. Fig.5 represents the rotor current as a function of the torque with unity inner power factor and with unity outer power factor respectively when the nominal stator flux linkage is used. In Fig.6 the load angles for two cases have been shown as a function of the torque.

Fig.5 points out that the rotor current value of inner control method is smaller than that of outer control method for the same torque point, and so it is advantageous to decrease the rotor copper losses if using the inner control scheme. The stable margin of load angle is larger under the condition of outer control method than that of inner control strategy as shown in Fig.6, and so the load ability of outer control method is increased.

The dependences between the air gap flux linkage and the torque are shown in Fig.7 for nominal stator flux linkage modulus. The value of air gap flux linkage is decreased when the torque is increased in the inner control strategy, and whereas on the contrary in the outer control strategy, which forces the magnetic circuit to be saturated.

TABLE I.
DATE OF MOTOR

Parameters	Values
Nominal power	300W
Nominal voltage	220V
Nominal speed	1500r.min ⁻¹
Pole pairs	2
d-axis inductance	0.9247H
q-axis inductance	0.604H
Multi-inductance between stator and rotor	0.45H
Stator resistance	13.3Ω
Rotor resistance	9.8Ω
Stator leakage inductance	0.1H
Rotor excited winding self inductance	0.4324H
Self inductance of d-axis damper winding	0.00356H
Resistance of d-axis damper winding	0.151Ω
Multi-inductance between d-axis damper winding and excited winding	0.028308H
Multi-inductance between d-axis damper winding and stator winding	0.04236H
Self inductance of q-axis damper winding	0.0032H
Resistance of q-axis damper winding	0.14Ω
Multi-inductance between q-axis damper winding and stator winding	0.031222H

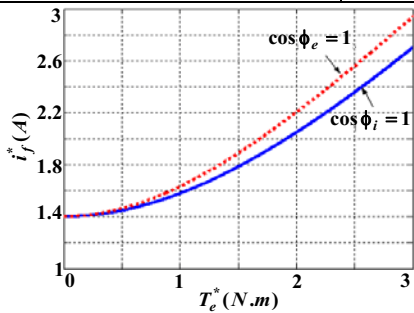


Figure 5. The relation between the rotor current and torque

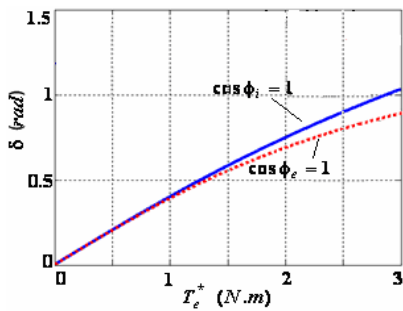


Figure 6. The relation between the load angle and torque

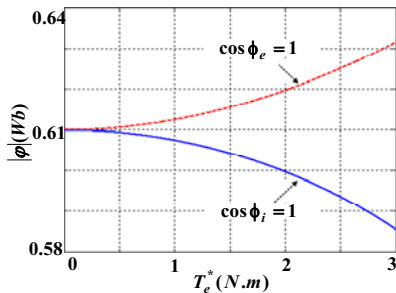


Figure 7. The relation between the air gap flux linkage modulus and the torque

The relations between the outer power factor and the torque under different speeds are shown in Fig.8. It is noticed in Fig.8 that the outer power factor is decreased when the torque is increased, whereas increased when the rotor speed is decreased. The lowest value 0.968 of outer power factor is achieved at the nominal speed, and the outer power factor decreases quickly when the torque increases above the nominal speed.

From the above analysis, the inner control method of rotor current is suited well under the nominal speed in order to decrease the rotor winding loss, while the outer control method is suited well above the nominal speed in order to increase the load ability. Therefore an optimum rotor current control strategy for DTC ESM drives is presented as shown in Fig.9. In the constant torque range below the nominal speed n_N , the inner control method of rotor current is adopted, and while the outer control strategy in the field weakening range with constant power.

IV. EXPERIMENTAL RESULTS

In order to compare the performances of basic DTC and SVM-DTC for ESMs, the sampling periods are all 100μs in the two DTC systems. The diagram of ESM SVM-DTC with sensorless technique is shown in Fig. 10.

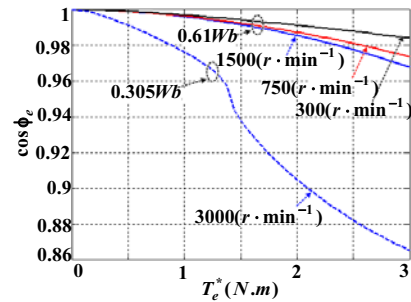


Figure 8. The relation between the outer power factor and torque

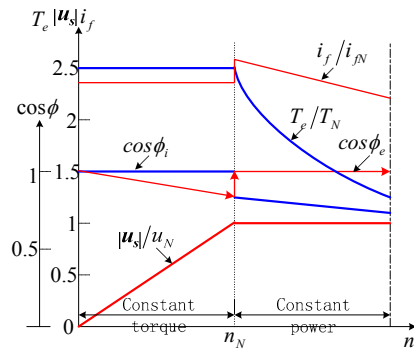


Figure 9. The presented optimum rotor current control strategy for DTC ESMs

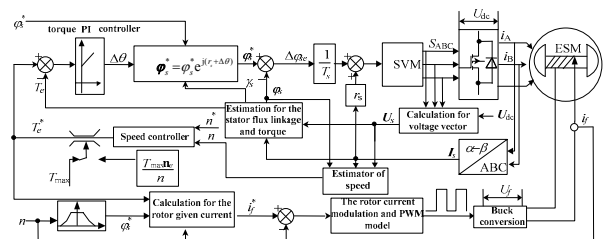


Figure 10. System diagram of the ESM SVM-DTC

The rotor field current is controlled using a buck conversion. The output variable of torque PI controller is the changing value of the torque angle θ .

The steady state phase currents of the two DTC schemes at the nominal speed $1500\text{r}\cdot\text{min}^{-1}$ with no load. The waveform of SVM-DTC is much smoother than that of basic DTC.

Fig.12 shows the torque and stator flux linkage waveforms of the two schemes at nominal speed with no load. The ripples of the torque and stator flux linkage in SVM-DTC are much smaller than those in basic DTC as shown in Fig.12.

In Fig.13, the torque dynamic responses of the two DTC schemes from $-3\text{N}\cdot\text{m}$ to $+3\text{N}\cdot\text{m}$ are researched. The torque response time of the SVM-DTC is almost the same as that of the basic DTC.

The experimental waveforms of field weakening operation are shown in Fig. 14. The rotor speed begins increasing from the point t_0 at $750\text{r}\cdot\text{min}^{-1}$. The speed is $1500\text{r}\cdot\text{min}^{-1}$ at the point t_1 and the stator flux linkage begins reducing from 0.61Wb as well as torque with $3\text{N}\cdot\text{m}$ from this point. The rotor field current increases from 3A to 3.5A at point t_1 from which motor begins working in the weakening range. At the point t_2 , the speed is $2000\text{r}\cdot\text{min}^{-1}$ and stator flux linkage is reduced to 0.45Wb . The weakening operation is included into SVM-DTC scheme well and ESM works very smoothly from above experimental waveforms.

The steady state waveforms at the $300\text{r}\cdot\text{min}^{-1}$ and $2000\text{r}\cdot\text{min}^{-1}$ with $1.5\text{N}\cdot\text{m}$ load are shown in Fig.15 and Fig.16 respectively. φ_α , i_α are the α -axis stator flux linkage and current in the stationary frame respectively. The flux linkage component φ_α lags the current component i_α near 90 electrical angle degrees as shown in Fig.15 and Fig.16. It is seen that the stator winding voltage leads the corresponding winding flux linkage 90 electrical angle degrees in the phase if neglecting the stator winding voltage drop. Therefore, the stator winding voltage and current are near in the same phase, and the outer power factor is equal to unity approximately using the presented optimum rotor field current control strategy.

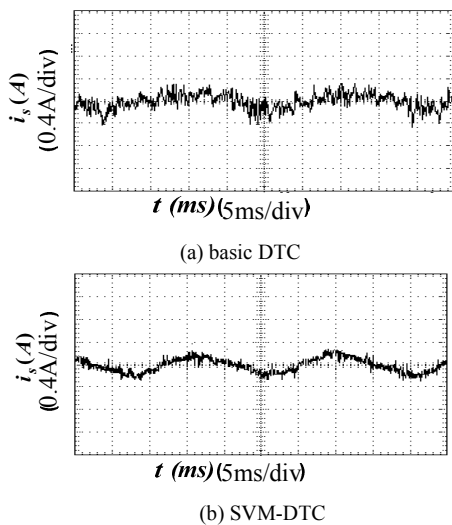


Figure 11. The experimental waveforms of phase current at $1500\text{r}\cdot\text{min}^{-1}$ with no load

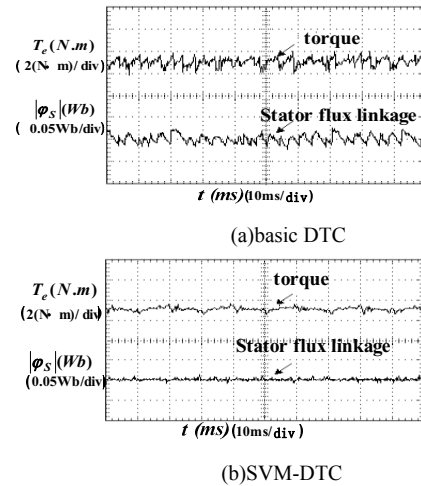


Figure 12. The experimental waveforms of torque and stator flux linkage at $1500\text{r}\cdot\text{min}^{-1}$ with no load

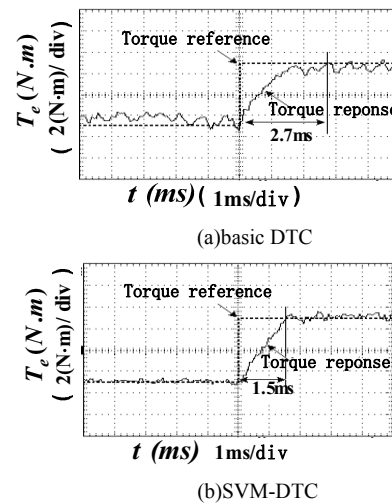


Figure 13. The experimental waveforms of torque step response

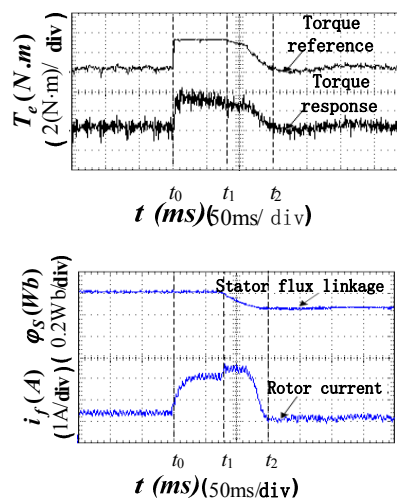
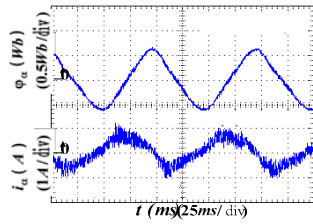
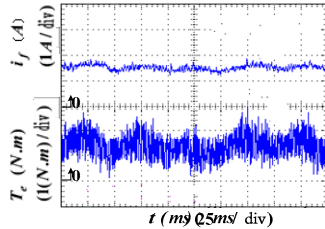


Figure 14. Field weakening operation from $750\text{r}\cdot\text{min}^{-1}$ to $2000\text{r}\cdot\text{min}^{-1}$

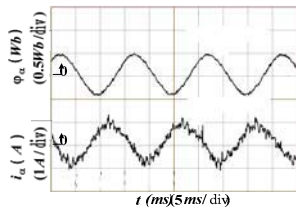


(a) α -axis stator flux linkage φ_α and current i_α

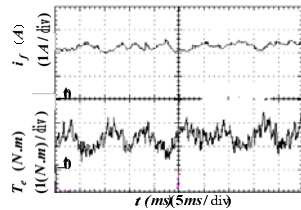


(b) rotor current i_f and torque T_e

Figure 15. the steady state experimental waveforms at the 3000r.min⁻¹ with 1.5N.m load



(a) α -axis stator flux linkage φ_α and current i_α



(b) rotor current i_f and torque T_e

Figure 16. the steady state experimental waveforms at the 2000r.min⁻¹ with 1.5N.m load

V. CONCLUSION

Compared with the basic DTC ESM drives, the SVM DTC drives have low ripples in torque and flux linkage,

and there are almost the same torque response speed in the two DTC methods.

In whole speed range, the outer power factor is almost equal to unity under the optimum rotor current control strategy presented in this paper. Quick rotor current response has been achieved in the transient state, and so the drive has better dynamic performance.

REFERENCES

- [1] Pyrhonen J, Niemela M, Kaukonen J et al. , "Synchronous motor drives based on direct flux linkage control," *Proceedings of the European Power Electronics Conference* , Norway: Trondheim, vol.1,pp. 434-439,1997.
- [2] Pyrhonen J, Niemela M, Kaukonen J et al. , "Test results with the direct flux linkage control of synchronous motors," *IEEE AES Systems Magazine* , vol.4, 1998,pp.23-270.
- [3] Casadei D, Serra G and Tani A. , "Constant frequency operation of a DTC induction motor drive for electric vehicle," *Proceedings of ICEM* , Spain:Vigo,vol.3,pp. 224-229,1996.
- [4] Xu L, Fu M. , "A novel sensorless control technique for permanent magnet synchronous motors(PMSM) using digital signal processor (DSP)," *Proceedings of Aerospace and Electronics Conference* , Ohio:Dayton,vol.1,pp. 403-406,1997.
- [5] Tang L X, Zhong L M, Rahman M F et al. , "A novel direct torque controlled interior permanent magnet synchronous machine drive with low ripple in flux and torque and fixed switching frequency," *IEEE Transactions on Power Electronics* , vol.19,no.2,2004, pp.346-354.
- [6] Yangzhong Zhou, Yuwen Hu, Jiao Tian, "Research of torque controller with variable proportion in permanent magnet synchronous motor drive," *Proceedings of the CSEE* , vol.24, no.9,2004, pp.204-208. (in Chinese)
- [7] Baader U. , "High dynamic torque control of induction motor in stator flux oriented coordinates," *ETZ Arch* , vol.11,no.1,1998, pp.11-17.
- [8] Habetler T G, Profumo F, Pastorelli M et al. ,Direct torque control of induction motor using space vector modulation, *IEEE Transaction on Industry Applications* , vol.28,no.5,1992, pp: 1045-1053.
- [9] Lascu C, Andrzej M T. , "Combining the principles of sliding mode, direct torque control, and space-vector modulation in a high- performance sensorless ac drive," *IEEE Transactions on Industry Applications* , vol.40,no.1,2004, pp: 170-177.
- [10] Yangzhong Zhou, Yuwen Hu, Wenxin Huang et al. , "Effect of damper windings on the dynamic performance of electrically excited synchronous motor based on direct torque control," *Acta Aeronautica et Astronautica Sinica* , vol.26,no.4,2005, pp.476-481. (in Chinese)